의학박사 학위논문

Evaluation of Antiangiogenic Effect Using Arterial Spin Labeling Perfusion MR Imaging in Rat Glioblastoma Model Treated with Bevacizumab

Bevacizumab 으로 치료한 랫드 교모세포종 모델에서의 동맥 스핀 표지 관류 자기공명영상을 이용한 혈관형성억제 효과의 평가

2016년 2월

서울대학교 대학원

의학과 영상의학 전공

윤 태 진

Evaluation of Antiangiogenic Effect Using Arterial Spin Labeling Perfusion MR Imaging in Rat Glioblastoma Model Treated with Bevacizumab

지도 교수 한 문 희

이 논문을 의학박사 학위논문으로 제출함
2016년 01월

서울대학교 대학원
의학과 영상의학 전공
윤 태 진

윤태진의 의학박사 학위논문을 인준함
2016년 01월

위 원 장 윤 병 우 (인)

부위원장 한 문 희 (인)

위 원 김 정 은 (인)

위 원 박 선 원 (인)

위 원 김 호 성 (인)

ABSTRACT

Background and Purpose– I evaluated the antiangiogenic effect of bevacizumab in a rat glioblastoma (GBM) model based on arterial spin labeling (ASL) perfusion MR imaging compared to dynamic susceptibility contrast (DSC) perfusion MR imaging with histopathology.

Materials and Methods– The protocol was approved by the institutional animal care and use committee. DSC and ASL perfusion MR imaging were performed using a 9.4 T MR scanner in nude rats with GBM. Rats were randomly assigned in the following three groups: control, 3-days treatment, and 10-days treatment. One-way analysis of variances was used to compare perfusion parameters (e.g. normalized cerebral blood volume [nCBV] from DSC MR imaging, and normalized cerebral blood flow [nCBF] based on DSC MR imaging and ASL MR imaging) with microvessel area (MVA) on histology Pearson's correlations between perfusion parameters and MVA were determined.

Results– MVA showed the consistent decrease with significant differences for the control, 3-days treatment, and 10-days treatment ($P < 0.001$). Consistent decreases with significant differences were also revealed in all perfusion parameters ($P < 0.05$ for all). In addition, nCBV and nCBF from DSC, and nCBF from ASL strongly correlated

with MVA (R^2 = 0.830, 0.755, and 0.739, respectively, $P < 0.001$ for all).

***Conclusions*–** nCBF based on ASL has the potential to be used to evaluate the effect of antiangiogenic therapy on GBMs treated with bevacizumab with strong correlation with MVA.

Keywords: Glioblastoma; Antiangiogenic effect; Bevacizumab; Dynamic susceptibility contrast; Arterial spin labeling

Student number: 2011-30568

CONTENTS

List of Tables

List of Figures

1. INTRODUCTION

Glioblastoma (GBM) is the most common primary malignant brain tumor in adults. Surgical tumor resection followed by radiation therapy and concurrent chemoradiotherapy with temozolomide is the current standard therapy for patients with GBM. [1] Despite multiple treatment approaches, however, the prognosis for patients with GBM is still extremely dismal. [2, 3]

GBMs are highly vascularized tumors and have been as attractive targets of antiangiogenic therapies. [4] In particular, vascular endothelial growth factor (VEGF) has been identified as a critical regulator of angiogenesis. Currently, a number of clinical trials targeting the VEGF-signaling pathways are under development. [5, 6] Bevacizumab is a recombinant humanized monoclonal antibody that binds to human VEGF and inhibits angiogenesis. [7] It received accelerated FDA approval for treating recurrent GBM in the United States and many other countries and has become the standard of care for treating GBM. [8, 9]

Dynamic susceptibility contrast (DSC) perfusion MR imaging can be used as a surrogate marker of perfusion to measure relative cerebral blood volume (rCBV) and relative cerebral blood flow (rCBF) of patients with GBM. [10-13] DSC perfusion MR imaging has shown the potential as an imaging biomarker to evaluate the antiangiogenic treatment in human GBM patients. [11-14] Some researchers have investigated the change in rCBV or rCBF in

animal GBM models and found significant reduction in animals treated with bevacizumab compared to controls. [15, 16] However, the correlation between perfusion parameters based on DSC perfusion MR imaging and microvascular environment in histological specimens in subjects treated with antiangiogenic therapy has not been elucidated.

Arterial spin labeling (ASL) technique is a promising perfusion MR imaging technique without using exogenous gadolinium based contrast agent for CBF quantification, in which the spin population in arterial water magnetically labeled by inversion is used as an endogenous diffusible tracer. [17, 18] Recent reports of ASL techniques applied to brain tumors have shown increased perfusion in pretreatment glioma. [19, 20] It has been suggested that ASL has the potential to evaluate the response to antiangiogenic therapy in patient with recurrent GBM received bevacizumab. [21]

Therefore, the objective of this study was to evaluate the antiangiogenic effect of bevacizumab in a rat GBM model based on ASL perfusion MR imaging relative to a more established technique based on DSC perfusion MR imaging with histopathology.

2. MATERIALS AND METHODS

2.1. Tumor cell line

Human glioma cells U87 (ATCC, Rockville, MD, USA) were cultured at 37°C in a humidified CO_2 incubator in RPMI medium supplemented with 10% fetal bovine serum.

2.2. Animal model

This study was approved by the Institutional Animal Care and Use Committee (IACUC) in Seoul National University Hospital (#12-0238-C1A0) and performed in accordance with institutional guidelines. Nude athymic rats (200–250 g; Koatec Inc, Gyeonggi-do, Korea) were anesthetized by intraperitoneal injection of a mixture of zolazepam and xylazine, and they were placed in a stereotaxic device. Nude rats were inoculated with U87 glioma cells (3×10^6 cells per 3 μL of serum-free RPMI medium) in the right caudate-putamen region. Cells were injected into the brain by using a Hamilton syringe fitted with a 28-gauge needle positioned with a syringe attachment fitted to the stereotaxic device. With stereotaxic guidance, 0 mm, 1.4 mm, and 3.0 mm were used in the posterior, lateral, and dorsal to the bregma in the right caudate-putamen, respectively.

Tumor growth was verified by MR imaging at 2 weeks after implantation. Animals were randomly assigned into control group (n = 4), 3-days treatment group (n = 6), and 10-days treatment group (n = 4). Control

animals were sacrificed for brain harvest right after the first MR imaging. For the 3- and 10-days treatment groups, bevacizumab was administered intraperitoneally at 20 mg/kg in saline right after the first MR imaging. [22] After 3 days, animals underwent the second MR imaging. Animals in the 3-days treatment group were sacrificed right after the second MR imaging. At 7 days post the second MR imaging, animals in the 10-days treatment group underwent the third MR imaging. They were sacrificed right after the third MR imaging. The *in vivo* experimental design of the present study is shown in Figure 1.

2.3. MRI acquisition

All MR image acquisitions were performed using a 9.4 T MR scanner (Agilent 9.4T/160AS; Agilent Technologies, Santa Clara, CA, USA). A volume coil for radiofrequency transmission and a phased-array 4 channel surface coil for signal reception (Agilent Technologies) were used.

Prior to MR image scans, animals were anesthetized with 1.5% isoflurane in room air and placed inside a magnet. Animals were physiologically monitored throughout MR experiments. To avoid potential changes in cerebral blood perfusion during data collection, their respiration was carefully maintained.

Following the acquisition of routine scout images in all three orthogonal directions, an automatic shimming procedure was performed.

Unenhanced anatomic T2-weighted images (T2WIs) were collected by using a fast spin echo sequence with the following parameters: repetition time (TR)/effective echo time (TE_{eff}) at 2000/45 ms, field of view (FOV) at 33 × 35 mm^2, matrix size at 256 × 256, echo train length at 4, 15 slices without gap, slice thickness (TH) at 1 mm, 1 signal average, 2 dummy scans, and receiver bandwidth (BW) at 100 kHz.

For perfusion data acquisition using ASL technique, an amplitude-modulated pseudo-continuous arterial spin labeling (pCASL) sequence was used with a single-shot spin-echo planar imaging readout (sineCASL; Agilent Technologies). [23] Vascular and fat suppression modules were also used with labeling pulse duration of 3 sec. Post-labeling delay and the gap between the labeling plane and the central imaging plane were 300 ms and 20 mm, respectively. Other sequence parameters were: TR/TE = 4000/28 ms, FOV = 33 × 35 mm^2, matrix size = 64 × 64, 3 slices, TH = 2 mm, BW = 250 kHz, and 60 repetitions for labeled and control data. For quantitative analysis of cerebral blood perfusion, T1 mapping was performed by using a fat-suppressed, single-shot, inversion-recovery spin-echo echo planar imaging sequence with TR = 8000 ms, and inversion times of 15, 35, 80, 200, 450, 1000, 2300, or 5400 ms. The rest of the sequence parameters were identical to those used for pCASL data acquisition. [23]

Finally, DSC images were acquired from the same imaging planes as for the pCASL experiments by using a gradient echo pulse sequence. The sequence parameters were: TR/TE at 25/5 ms, flip angle at 10°, matrix size of

128 × 96, 4 signal averages, BW at 100 kHz, and 70 repetitions. After an initial 30-second baseline acquisition, a bolus of gadoterate meglumine (0.1 mmol per kilogram of body weight; Dotarem®, Guerbet, Aulnay-sous-Bois, France) was administered into animals via tail vein catheter using a syringe pump (1 mL/min; Harvard Apparatus, Holliston, MA) which was immediately followed by a 1 mL saline flush.

2.4. MRI data analysis

All pCASL images were analyzed using Matlab (Math Works, Inc., Natick, MA, USA). CBF maps were derived according to previous reports. [23, 24] A three-parameter fit was used for estimating T1 maps. Once T1 maps and control as well as labeled images were obtained, tissue blood flow images were formed according to the following formula: $CBF = (\lambda/T1) \times (S_{control} - S_{label}) / (2\alpha \times S_{control})$, where $\lambda = 0.9$ was tissue: blood partition coefficient for water, [24] $S_{control}$ was control image signal intensity, S_{label} was labeled image signal intensity, T1 was T1 map, and α was 0.63 as the degree of labeling efficiency. [23]

For DSC perfusion MR, additional preprocessing was performed by using commercialized software (Nordic ICE, NordicNeuroLab, Bergen, Norway), in which T2WIs were used for structural imaging. rCBV maps were generated by using established tracer kinetic models applied to first-pass data. [25, 26] To reduce the effect of recirculation, $\Delta R2^*$ ($1/T2^*$) curves were fitted to

gamma-variate function which was an approximation of the first pass response as it would appear in the absence of recirculation or leakage. The dynamic curves were mathematically corrected to reduce contrast-agent leakage effects. [27]

T2WI, rCBV and rCBF maps based on DSC, and CBF maps based on ASL were analyzed by using commercialized PACS console (Infinite PACS viewer, Infinite, Korea). I who was blinded to experimental data drew ROIs containing the entire tumor in the plane in which the tumor area was the largest. Tumor boundaries were defined with reference to high-signal intensity areas thought to represent tumor tissue on the T2WI. [15, 16] To include the enhancing and non-enhancing portions of GBM and overcome the possible bias due to the effect on the enhancement pattern of GBM following the antiangiogenic therapy, T2WI-based ROI was defined in the present study. ROIs were copied and placed to co-registered rCBV and rCBF maps based on DSC and CBF map from ASL. Mean rCBV and mean rCBF of each tumor were measured on rCBV and rCBF maps. Mean rCBV and mean rCBF of contralateral hemisphere were also measured as references values for perfusion parameters. Normalized CBV (nCBV) and normalized CBF (nCBF) were derived using the following formula: $nCBV = rCBV_{tumor} / rCBV_{reference}$, $nCBF = rCBF_{tumor} / rCBF_{reference}$ (Figure 2).

2.5. Histological analysis

All rats were euthanized in CO_2 chamber soon after MR imaging. Coronal sections sampled across the center of tumors were fixed in 10% buffered formaldehyde solution and paraffin embedded. Coronal paraffin sections were used for histological hematoxylin/eosin staining and immunohistochemical analysis. Histological evaluation was performed using a standard light microscope. Microvascular area (MVA) was determined based on CD34 immunostains. First, CD34-stained sections were scanned at low magnifications. And, the tumor area with the highest density of highlighted microvessels was selected around the center of the tumor avoiding the portions including necrosis and hemorrhage. Finally, MVA consisting of endothelial area and vessel lumen were quantified with a higher power (× 200 field) in the selected area. [28, 29] Results were expressed as the ratio of the area of microvessel to the total area of analysis within any single 200× microscopic field.

2.6. Statistical analysis

Paired and unpaired t-tests were used to compare parameters on perfusion MR imaging and MVA on histology within subjects and between groups. For tumors in which histology were available, one-way analysis of variance was used to analyze differences. Pearson's correlation analysis was performed to determine the correlation among perfusion parameters of

perfusion MR imaging and MVA. Statistical analysis was performed with commercially available software SPSS (version 12.0 for Windows, Chicago, Ill, USA) and MedCalc (v 9.3.0.0, MedCalc Software, Mariakerke, Belgium). Statistical significance was considered when *P* value was less than 0.05. With Bonferroni correction to adjust for multiple comparisons, statistically significant difference was considered when *P* value was less than 0.0125.

3. RESULTS

3.1. Analysis of tumor volume and perfusion parameters based on DSC or ASL perfusion MR imaging in all tumors

The changes of tumor volume and perfusion parameters in all tumors before and after bevacizumab treatment are summarized in the Tables 1 and 2.

Two weeks after implantation of U87 glioma cells, the median value of initial tumor size of animals (n = 14) before treatment (0 days) was 40.0 mm^3 with [interquartile range from the 25th to the 75th percentile of 32.3-61.8 mm^3] (values are reported as median value [range from the 25th to the 75th percentile], unless otherwise specified) determined from visible part (tumor core) of T2WIs. After bevacizumab treatment, a tendency of consistent increase in tumor volume was revealed on unpaired t-test (in which P-value less than 0.1) (Figure 3).

Initial nCBV based on DSC MR imaging of all tumors before treatment was 5.9 [5.7-6.3]. After 3 days of treatment, nCBV of all tumors in combined 3- and 10-days treatment groups was 2.7 [2.4-2.9]. The nCBV of tumors in the 10-days treatment group was 0.8 [0.6-1.4] at 10 days after treatment. All P values based on paired t-test and unpaired t-test between two groups were less than 0.0125. Initial nCBF from DSC MR imaging of tumors before treatment was 3.7 [3.2-4.0]. After 3 days of treatment, nCBF of all

tumors in combined 3- and 10-days treatment groups was 1.8 [1.4-2.2]. For tumors in the 10-days treatment group, the nCBF was 0.7 [0.6-1.0]. P values based on paired t-test and unpaired t-test between two groups were less than 0.0125 except for paired and unpaired t-test between 0 days and 3 days after treatment or between 0 days and 10 days after treatment (P = 0.020 and 0.075, respectively). Initial nCBF based on ASL before treatment was 1.7 [1.2-2.0]. After 3 days of treatment, nCBF of all tumors in the combined 3- and 10-days treatment groups was 0.3 [0.2-0.5]. For the 10-days treatment group, the nCBF was 0.1 [0.1-0.1]. P values based on paired t-test and unpaired t-test among groups were less than 0.0125 except for that between 0 days and 3 days after treatment (P = 0.041 and 0.050, respectively) (Figure 3).

3.2. Analysis of tumor volume and perfusion parameters based on DSC and ASL perfusion MR imaging as well as MVA in tumors with available histology

Comparison and correlation of tumor volume and perfusion parameters from DSC and ASL perfusion MR imaging as well as MVA in tumors with available histology are summarized in Table 3.

According to one-way analysis of variance, MVA of the control group (n = 4), 3-days treatment group (n = 6), and 10-days treatment group (n = 4) were 0.075 [0.069-0.079], 0.028 [0.023-0.033], and 0.024 [0.019-0.029],

respectively, with significant ($P < 0.001$) difference among them. Scheffe's post-hoc multiple comparisons revealed significant ($P < 0.05$) difference between the control group and the 3-days treatment group as well as between control and the 10-days treatment group (Figure 4).

There was a tendency of consistent increase in tumor volume with P-value less than 0.1 ($P = 0.066$). However, there were significant differences in all perfusion parameters (nCBV from DSC, nCBF from DSC, and nCBF from ASL, $P < 0.001$, $P < 0.001$, and $P = 0.005$, respectively). Scheffe's post-hoc multiple comparisons revealed significant ($P < 0.05$) differences between the control group and the 3-days treatment group as well as between control and the 10-days treatment in all perfusion parameters. In addition, significant ($P < 0.05$) difference was found between the 3-days treatment group and the 10-days treatment group in nCBV from DSC (Figure 4).

In tumors with available histology ($n = 14$), nCBV and nCBF based on DSC, and nCBF based on ASL significantly ($P < 0.001$) correlated with MVA ($R^2 = 0.830$, 0.755, and 0.739, respectively). nCBF from ASL perfusion MR imaging also had a positive and significant ($P < 0.001$) correlation with nCBF and nCBV based on DSC MR imaging ($R^2 = 0.688$ and 0.622, respectively) (Figure 5). However, nCBF (0.2 [0.1-0.6]) measured on ASL perfusion MR imaging was significantly ($P < 0.001$) less than that (1.9 [1.4-3.0]) based on DSC MR imaging.

Table 1. Volume and perfusion parameters for tumors based on DSC and ASL MR imaging in all tumors

Groups	Volume (mm^3)			$nCBV_{DSC}$			$nCBF_{DSC}$			$nCBF_{ASL}$		
	0 days	3 days	10 days	0 days	3 days	10 days	0 days	3 days	10 days	0 days	3 days	10 days
Control												
A1	62.1			5.3			3.1			0.2		
A2	38.4			6.6			3.6			2.1		
A3	102.1			6.2			4.2			1.3		
A4	41.6			5.9			3.3			1.6		
3-days treatment												
B1	56.7	107.1		5.0	2.5		3.2	1.8		2.0	0.2	
B2	37.5	92.2		6.0	2.3		3.7	1.5		0.4	0.1	
B3	12.7	25.2		5.8	2.8		2.9	1.9		0.4	0.3	
B4	60.9	91.6		7.5	4.1		4.1	2.7		2.1	0.6	
B5	85.8	133.8		6.1	2.2		3.7	1.8		1.2	0.6	
B6	80.4	129.8		6.7	1.9		4.6	1.4		1.9	0.2	
10-days treatment												
C1	35.4	55.2	287.2	5.6	2.7	0.5	2.9	1.2	0.6	1.3	0.5	0.1

C2	29.0	53.5	120.2	5.6	4.0	2.6	3.8	1.2	2.0	4.9	0.6	0.1
C3	27.4	35.9	51.3	5.2	3.0	1.0	3.3	1.3	0.6	1.9	0.4	0.1
C4	31.3	137.2	343.4	6.4	2.7	0.6	4.0	1.4	0.7	2.3	0.2	0.0

- $nCBV_{DSC}$: nCBV based on DSC; $nCBF_{DSC}$: nCBF based on DSC; $nCBF_{ASL}$: nCBF based on ASL.

Table 2. Comparison of tumor volume and perfusion parameters of tumors based on DSC and ASL MR imaging in all tumors

Variables	0 days (n = 14)	3 days (n = 10)	10 days (n = 4)	Paired t-test			Unpaired t-test		
				P value*	P value†	P value‡	P value*	P value†	P value‡
Volume (mm^3)	40.0 [32.3-61.8]	91.9 [53.9-124.1]	203.7 [103.0-301.3]	0.015	0.200	0.117	0.002	0.090	0.086
$nCBV_{DSC}$	5.9 [5.7-6.3]	2.7 [2.4-2.9]	0.8 [0.6-1.4]	< 0.001	0.004	< 0.001	< 0.001	0.002	0.005
$nCBF_{DSC}$	3.7 [3.2-4.0]	1.8 [1.4-2.2]	0.7 [0.6-1.0]	< 0.001	0.020	< 0.001	< 0.001	0.075	0.004
$nCBF_{ASL}$	1.7 [1.2-2.0]	0.3 [0.2-0.5]	0.1 [0.1-0.1]	< 0.001	0.041	< 0.001	0.004	0.029	0.050

-Values are presented as median value [interquartile range, range from the 25th to the 75th percentile].

- $nCBV_{DSC}$: nCBV based on DSC; $nCBF_{DSC}$: nCBF based on DSC; $nCBF_{ASL}$: nCBF based on ASL.

*; Results between 0 day and 3 days.

†; Results between 3 days and 10 days

‡; Results between 0 day and 10 days.

Table 3. Comparison and correlation of perfusion parameters based on DSC and ASL MR imaging with MVA in tumors with available histology

Variables	Control (n = 4)	3-days treatment (n = 6)	10-days treatment (n = 4)	*P* value*	Different groups†
Volume (mm^3)	51.9 [40.8-72.1]	99.7 [91.8-124.1]	203.7 [103.0-301.3]	0.066	
$nCBV_{DSC}$	6.0 [5.7-6.3]	2.4 [2.2-2.7]	0.8 [0.6-1.4]	< 0.001	(Control)(3-days), (3-days)(10-days) (Control)(10-days)
$nCBF_{DSC}$	3.5 [3.3-3.7]	1.8 [1.5-1.9]	0.7 [0.6-1.0]	< 0.001	(Control)(3-days), (Control)(10-days)
$nCBF_{ASL}$	1.4 [1.0-1.7]	0.3 [0.2-0.5]	0.1 [0.1-0.1]	0.005	(Control)(3-days), (Control)(10-days)
MVA ($x10^{-2}$)	7.5 [6.9-7.9]	2.8 [2.3-3.3]	2.4 [1.9-2.9]	< 0.001	(Control)(3-days), (Control)(10-days)

-Values are presented as median value [interquartile range, range from the 25th to the 75th percentile].

- $nCBV_{DSC}$: nCBV based on DSC; $nCBF_{DSC}$: nCBF based on DSC; $nCBF_{ASL}$: nCBF based on ASL.

*; Results from one-way analyses of variances.

†; Results from Scheffe's post-hoc multiple comparisons.

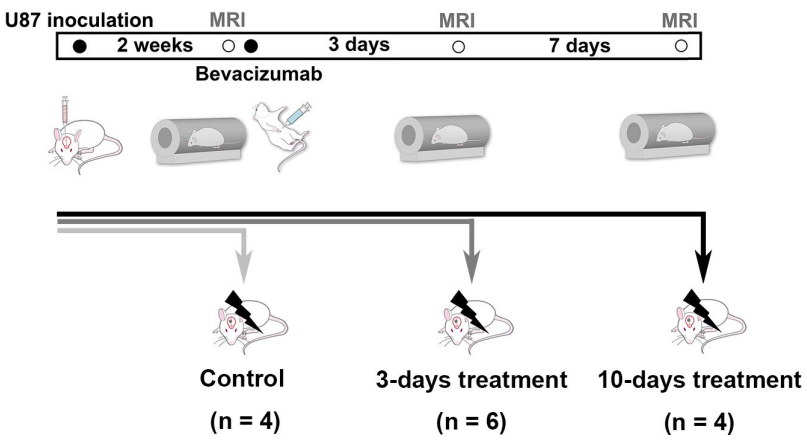

Figure 1. Experimental design showing the timeline of each group for U87 glioma cells inoculation, bevacizumab therapy, MR imaging, and sacrifice for brain harvest.

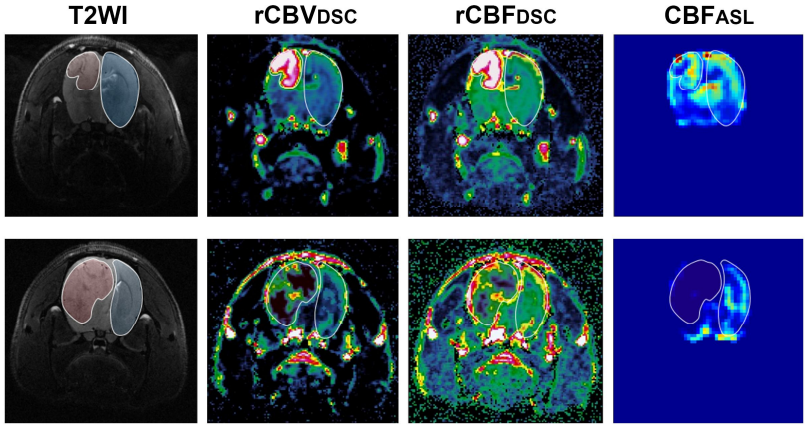

Figure 2. Representative images showing how to define region of interest (ROI).

First, tumor boundaries were defined as high-signal intensity areas thought to represent tumor tissue on the T2WIs. ROIs were copied and placed to co-registered rCBV and rCBF maps based on DSC as well as CBF maps based on ASL. As references for perfusion parameters in ROIs, perfusion parameters in the contralateral hemisphere were also measured. T2WI: T2-weighted image; $rCBV_{DSC}$: rCBV based on DSC; $rCBF_{DSC}$: rCBF based on DSC; CBF_{ASL}: CBF based on ASL.

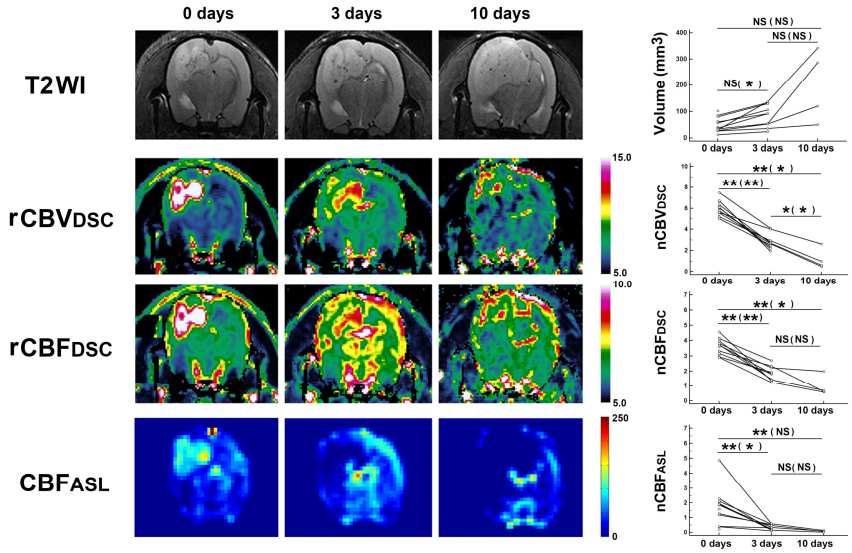

Figure 3. Quantification of tumor volume and perfusion parameters in all tumors.

T2WI and perfusion maps were acquired from a rat belonging to 10-days treatment group. Serial reductions in rCBV and rCBF based on DSC as well as CBF based on ASL are shown. Graphs in the right column show serial change of tumor volume and perfusion parameters in all tumors. $rCBV_{DSC}$: rCBV based on DSC; $rCBF_{DSC}$: rCBF based on DSC; CBF_{ASL}: CBF based on ASL. $nCBV_{DSC}$: nCBV based on DSC; $nCBF_{DSC}$: nCBF based on DSC; $nCBF_{ASL}$: nCBF based on ASL. Scale unit of $rCBV_{DSC}$, $rCBF_{DSC}$, and CBF_{ASL} are $mL \cdot 100\ g^{-1}$, $mL \cdot 100\ g^{-1} \cdot min^{-1}$, and $mL \cdot 100\ g^{-1} \cdot min^{-1}$, respectively. Data (data) means results from paired t-tests (unpaired t-tests). *: $P < 0.0125$; **: $P < 0.001$; NS: not significant.

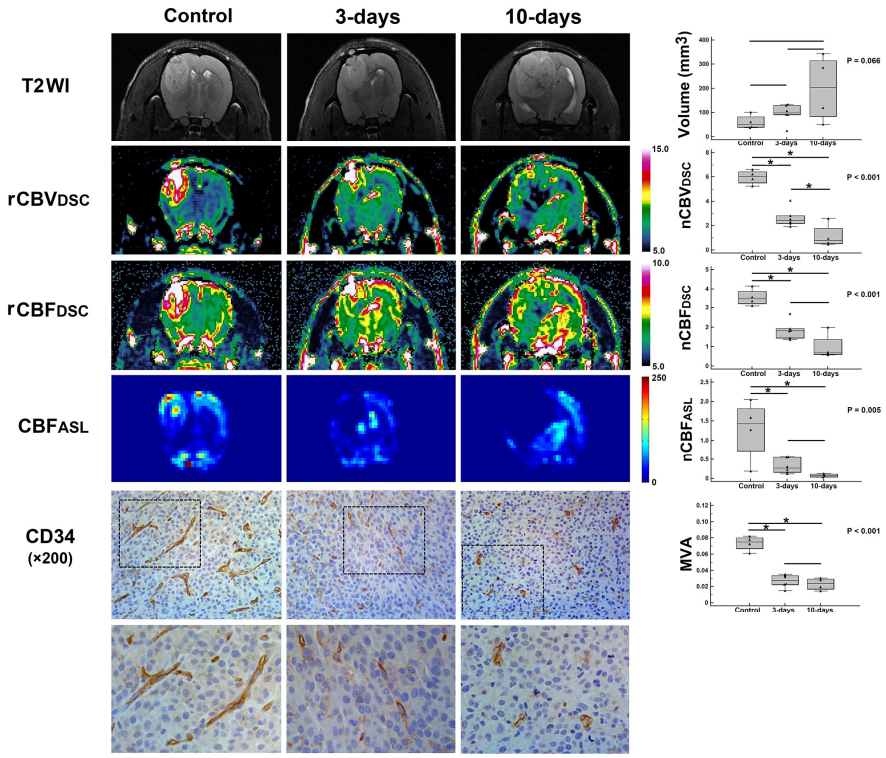

Figure 4. Quantification of tumor volume, perfusion parameters, and MVA in tumors with available histology.

T2WI and perfusion maps were acquired from rats in the control group, 3-days treatment group, or the 10-days treatment group. Differences in rCBV and rCBF based on DSC, CBF based on ASL, and MVA are shown. Graphs in the right column show differences in the tumor volume and hemodynamic parameters MVA. $rCBV_{DSC}$: rCBV based on DSC; $rCBF_{DSC}$: rCBF based on DSC; CBF_{ASL}: CBF based on ASL. $nCBV_{DSC}$; nCBV based on DSC; $nCBF_{DSC}$: nCBF based on DSC; $nCBF_{ASL}$: nCBF based on ASL. MVA: microvessel area. Scale unit of $rCBV_{DSC}$, $rCBF_{DSC}$, and CBF_{ASL} are $mL \cdot 100\ g^{-1}$, $mL \cdot 100\ g^{-1} \cdot min^{-1}$, and $mL \cdot 100\ g^{-1} \cdot min^{-1}$, respectively. P values were based

on one-way analyses of variances. *: significant ($P < 0.05$) difference from Scheffe's post-hoc multiple comparisons.

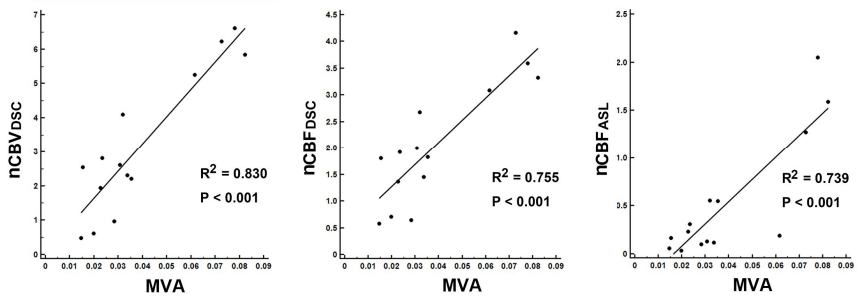

Figure 5. Correlations between perfusion parameters and MVA in tumors with available histology.

Significant positive correlations are shown between perfusion parameters and MVA. $nCBV_{DSC}$: nCBV based on DSC; $nCBF_{DSC}$: nCBF based on DSC; $nCBF_{ASL}$: nCBF based on ASL. MVA: microvessel area.

4. DISCUSSION

In the present study, I assessed the serial changes of perfusion parameters in a GBM rat model treated with antiangiogenic agent bevacizumab based on DSC and ASL perfusion MR imaging. I found that perfusion parameters based on ASL as well as DSC perfusion MR imaging decreased after antiangiogenic treatment, which correlated well with histopathology results such as MVA.

Since bevacizumab has been reported to have antiangiogenic effect in GBM and approved as a treatment agent either alone or in combination with chemotherapy, [6, 8] the potential of perfusion MR imaging to precisely characterize the microvascular environment has been clinically relevant. However, it was unclear whether perfusion MR imaging can be applied as an imaging biomarker to quantify the microvascular environment mainly due to significant intra- and inter-tumoral biological heterogeneity of GBM. Although some researchers have investigated the potential of DSC perfusion MR imaging in GBM treated with bevacizumab in animal models, [15, 30] direct correlation between perfusion parameters and histological features was not elucidated. In terms of ASL perfusion MR technique, a previous report has suggested the potential of using ASL perfusion MR imaging to evaluate the response to antiangiogenic therapy in a patient with recurrent GBM who received bevacizumab. [21] However, additional investigation in human study or animal model has not been elucidated.

According to the present results, nCBV and nCBF values based on DSC showed significant serial reduction after bevacizumab treatment with strong correlation with MVA in histology. Thus, they have the potential as imaging biomarkers to evaluate the antiangiogenic effect in GBM treated with bevacizumab. In addition, our results revealed that nCBF value based on ASL technique has significant serial reduction after bevacizumab treatment with strong correlation with MVA.

ASL perfusion MR technique has been recently incorporated as a part of the imaging tools to evaluate the measure cerebral perfusion at the tissue level. In ASL perfusion MR imaging, the labeled arterial blood water acts as a diffusible tracer to provide blood flow measurements in a manner analogous to that used for proton emission tomography. The primary advantage of using ASL for perfusion measurement is that this technique is completely non-invasive and does not expose the patient to radiation or contrast agents. [31] Therefore, ASL perfusion MR technique may enable characterization of microvascular environment and evaluation of the antiangiogenic effect against GBM in patients who have contraindications to contrast administration. However, in the clinical setting, usage of the contrast agent tends to be accepted as a prerequisite for the evaluation of GBM in most cases, unless the patients have contraindications to contrast administration. Therefore, the practical benefit of ASL perfusion MR imaging over DSC perfusion MR imaging may be less apparent in the clinical setting.

Many previous reports have indicated the possible advance in the evaluation of gliomas using ASL perfusion MR imaging. First, ASL perfusion MR imaging can contribute to the preoperative tumor evaluation including grading. Warmuth et al. quantified the tumor blood flow in patients with brain gliomas and found that high- and low grade gliomas can be distinguished using the perfusion parameter based on ASL. [20] In addition, Yoo et al. reported that tumor blood flow based on ASL may facilitate differentiation of high-grade gliomas from lymphomas. [32] Second, ASL perfusion MR parameter can predict the histopathologic vascular densities of gliomas. A few previous studies have shown a significant correlations between the ASL perfusion MR perfusion parameter and microvessel area or density in brain tumors including gliomas. [33, 34] Third, ASL perfusion MR parameter can be used as an indicator for the progression-free survival in patients with glioblastoma. [35] Finally, ASL perfusion MR imaging has been shown to be helpful for the differentiation between the recurrence and radiation necrosis and for the identification of pseudoprogression after or during the treatment. [36, 37]

I anticipate that the results of the present study, which demonstrated the potential of the ASL perfusion MR parameter as an imaging biomarker for monitoring the antiangiogenic effect in GBM, may facilitate the application of this technique for treatment monitoring of GBM.

Although there have been some previous studies that investigated the potential of the perfusion MR parameters as imaging biomarkers to evaluate the efficacy of antiangiogenic treatment in human GBM patients, [11-14] or in animals, [15, 16] those studies focused primarily on DSC perfusion MR imaging. However, radiation therapy that constitutes the current standard treatment for GBM can induce the breakdown of the blood-brain barrier and vascular leakage. [38] Therefore, when quantifying the cerebral perfusion using DSC perfusion MR imaging, the hemodynamic parameters such as CBV and CBF can be compromised by elevated vascular permeability and leakage of contrast agent, both of which can be heavily influenced by biological changes in GBM under treatment. [39] In addition, the susceptibility artifact due to intratumoral hemorrhage, which frequently occurs in GBM at its natural course or during the treatment, can be a drawback of the DSC perfusion MR imaging because DSC perfusion MR is sensitive to the susceptibility artifact. [40]

In contrast with the DSC perfusion MR imaging, the labeled arterial blood water acts as a diffusible tracer to allow blood flow measurements at the brain tissue level in ASL perfusion MR imaging. Therefore, ASL perfusion MR technique would be less sensitive to the breakdown of the blood-brain barrier and vascular leakage. [20] In addition, theoretically, ASL perfusion MR imaging is not based on the susceptibility effect. Therefore,

ASL may be a better perfusion technique for quantification of the perfusion in GBM, as compared with the DSC perfusion MR imaging.

However, nCBF value based on ASL perfusion MR imaging had a significantly lower value compared to that based on DSC. Leakage of contrast agent on DSC and insufficient labeling efficacy due to unestablished post-labeling decay time in animal models may contribute to the difference in nCBF values based on DSC and ASL. Since the appropriate post-labeling decay time has been established for brain imaging in humans, such discrepancy may be minimized in the application of ASL perfusion MR imaging for human GBM. Even though nCBV values based on DSC perfusion MR imaging had significant difference in animals between the 3-days treatment and 10-days treatment groups, no significant difference in MVA value was found between the two groups. Therefore, perfusion parameters based on DSC perfusion MR imaging might have been influenced by other factors related to the antiangiogenic mechanism beyond MVA.

Interestingly, the present study revealed a tendency of consistent increase in tumor volume despite reduced nCBV and nCBF values (in which P-value less than 0.1). Although we used 20 mg/kg of bevacizumab in this study based on a previous report that investigated its dose-dependent effect on GBM blood vessels, [22] the tumor volume showed serial increase in all tumors. Our result is consistent with previsions reports, [15, 22] suggesting a possible

insufficient effect of antiangiogenic therapy on tumor proliferation and/or possible evasion mechanism against antiangiogenic drug in GBM.

A shortcoming of the present study is the absence of untreated control groups at day 3 and day 10. Rats sacrificed at day 0 prior to treatment were designated as the sole control group, because the purpose of this study was to evaluate the antiangiogenic effect of bevacizumab in a rat GBM model using ASL or DSC perfusion MR imaging with histopathology as the reference standard,. Additional control groups in which the rats are untreated and followed for three and ten days would be helpful for assessing the perfusion status during the natural course of GBM.

In summary, **CBF value based on ASL has a good performance for evaluating antiangiogenic therapy with strong correlations with MVA in a rat GBM model. In addition, ASL perfusion MR imaging can overcome the drawbacks in DSC perfusion MR imaging including the vascular leakage and sensitivity to the susceptibility artifact. Therefore, ASL has a potential to be used as a non-invasive imaging biomarkers to monitor the effect of antiangiogenic therapy for GBMs.**

6. REFERENCES

1. Stupp R, Mason WP, van den Bent MJ, et al. Radiotherapy plus concomitant and adjuvant temozolomide for glioblastoma. *The New England journal of medicine* 2005;352:987-996

2. Erpolat OP, Akmansu M, Goksel F, et al. Outcome of newly diagnosed glioblastoma patients treated by radiotherapy plus concomitant and adjuvant temozolomide: a long-term analysis. *Tumori* 2009;95:191-197

3. Jeon HJ, Kong DS, Park KB, et al. Clinical outcome of concomitant chemoradiotherapy followed by adjuvant temozolomide therapy for glioblastaomas: single-center experience. *Clinical neurology and neurosurgery* 2009;111:679-682

4. Jain RK, di Tomaso E, Duda DG, et al. Angiogenesis in brain tumours. *Nature reviews Neuroscience* 2007;8:610-622

5. Miletic H, Niclou SP, Johansson M, et al. Anti-VEGF therapies for malignant glioma: treatment effects and escape mechanisms. *Expert opinion on therapeutic targets* 2009;13:455-468

6. Vredenburgh JJ, Desjardins A, Herndon JE, 2nd, et al. Phase Ⅱ trial of bevacizumab and irinotecan in recurrent malignant glioma. *Clinical cancer research : an official journal of the American Association for Cancer Research* 2007;13:1253-1259

7. Reardon DA, Turner S, Peters KB, et al. A review of VEGF/VEGFR-targeted therapeutics for recurrent glioblastoma. *Journal of the National*

Comprehensive Cancer Network : JNCCN 2011;9:414-427

8. Friedman HS, Prados MD, Wen PY, et al. Bevacizumab alone and in combination with irinotecan in recurrent glioblastoma. *Journal of clinical oncology : official journal of the American Society of Clinical Oncology* 2009;27:4733-4740

9. Kreisl TN, Kim L, Moore K, et al. Phase Ⅱ trial of single-agent bevacizumab followed by bevacizumab plus irinotecan at tumor progression in recurrent glioblastoma. *Journal of clinical oncology : official journal of the American Society of Clinical Oncology* 2009;27:740-745

10. Artzi M, Blumenthal DT, Bokstein F, et al. Classification of tumor area using combined DCE and DSC MRI in patients with glioblastoma. *Journal of neuro-oncology* 2015;121:349-357

11. Harris RJ, Cloughesy TF, Hardy AJ, et al. MRI perfusion measurements calculated using advanced deconvolution techniques predict survival in recurrent glioblastoma treated with bevacizumab. *Journal of neuro-oncology* 2015;122:497-505

12. Schmainda KM, Prah M, Connelly J, et al. Dynamic-susceptibility contrast agent MRI measures of relative cerebral blood volume predict response to bevacizumab in recurrent high-grade glioma. *Neuro-oncology* 2014;16:880-888

13. Stadlbauer A, Pichler P, Karl M, et al. Quantification of serial changes in cerebral blood volume and metabolism in patients with

recurrent glioblastoma undergoing antiangiogenic therapy. *European journal of radiology* 2015;84:1128-1136

14. Sawlani RN, Raizer J, Horowitz SW, et al. Glioblastoma: a method for predicting response to antiangiogenic chemotherapy by using MR perfusion imaging--pilot study. *Radiology* 2010;255:622-628

15. Jalali S, Chung C, Foltz W, et al. MRI biomarkers identify the differential response of glioblastoma multiforme to anti-angiogenic therapy. *Neuro-oncology* 2014;16:868-879

16. Keunen O, Johansson M, Oudin A, et al. Anti-VEGF treatment reduces blood supply and increases tumor cell invasion in glioblastoma. *Proceedings of the National Academy of Sciences of the United States of America* 2011;108:3749-3754

17. Detre JA, Alsop DC. Perfusion magnetic resonance imaging with continuous arterial spin labeling: methods and clinical applications in the central nervous system. *European journal of radiology* 1999;30:115-124

18. Detre JA, Leigh JS, Williams DS, et al. Perfusion imaging. *Magnetic resonance in medicine* 1992;23:37-45

19. Gaa J, Warach S, Wen P, et al. Noninvasive perfusion imaging of human brain tumors with EPISTAR. *European radiology* 1996;6:518-522

20. Warmuth C, Gunther M, Zimmer C. Quantification of blood flow in brain tumors: comparison of arterial spin labeling and dynamic susceptibility-weighted contrast-enhanced MR imaging. *Radiology*

2003;228:523-532

21. Fellah S, Girard N, Chinot O, et al. Early evaluation of tumoral response to antiangiogenic therapy by arterial spin labeling perfusion magnetic resonance imaging and susceptibility weighted imaging in a patient with recurrent glioblastoma receiving bevacizumab. *Journal of clinical oncology : official journal of the American Society of Clinical Oncology* 2011;29:e308-311

22. von Baumgarten L, Brucker D, Tirniceru A, et al. Bevacizumab Has Differential and Dose-Dependent Effects on Glioma Blood Vessels and Tumor Cells. *Clinical Cancer Research* 2011;17:6192-6205

23. Utting JF, Thomas DL, Gadian DG, et al. Understanding and optimizing the amplitude modulated control for multiple-slice continuous arterial spin labeling. *Magnetic resonance in medicine* 2005;54:594-604

24. Silva AC, Kim SG, Garwood M. Imaging blood flow in brain tumors using arterial spin labeling. *Magnetic resonance in medicine* 2000;44:169-173

25. Maeda M, Itoh S, Kimura H, et al. Tumor vascularity in the brain: evaluation with dynamic susceptibility-contrast MR imaging. *Radiology* 1993;189:233-238

26. Rollin N, Guyotat J, Streichenberger N, et al. Clinical relevance of diffusion and perfusion magnetic resonance imaging in assessing intra-axial brain tumors. *Neuroradiology* 2006;48:150-159

27. Aronen HJ, Gazit IE, Louis DN, et al. Cerebral blood volume maps of gliomas: comparison with tumor grade and histologic findings. *Radiology* 1994;191:41-51

28. Barbareschi M, Gasparini G, Morelli L, et al. Novel methods for the determination of the angiogenic activity of human tumors. *Breast cancer research and treatment* 1995;36:181-192

29. Nico B, Benagiano V, Mangieri D, et al. Evaluation of microvascular density in tumors: pro and contra. *Histology and histopathology* 2008;23:601-607

30. Keunen O, Taxt T, Gruner R, et al. Multimodal imaging of gliomas in the context of evolving cellular and molecular therapies. *Advanced drug delivery reviews* 2014;76:98-115

31. Wolf RL, Detre JA. Clinical neuroimaging using arterial spin-labeled perfusion magnetic resonance imaging. *Neurotherapeutics* 2007;4:346-359

32. Yoo RE, Choi SH, Cho HR, et al. Tumor blood flow from arterial spin labeling perfusion MRI: a key parameter in distinguishing high-grade gliomas from primary cerebral lymphomas, and in predicting genetic biomarkers in high-grade gliomas. *J Magn Reson Imaging* 2013;38:852-860

33. Noguchi T, Yoshiura T, Hiwatashi A, et al. Perfusion imaging of brain tumors using arterial spin-labeling: correlation with histopathologic vascular density. *AJNR American journal of neuroradiology* 2008;29:688-

693

34. Weber MA, Zoubaa S, Schlieter M, et al. Diagnostic performance of spectroscopic and perfusion MRI for distinction of brain tumors. *Neurology* 2006;66:1899-1906

35. Qiao XJ, Ellingson BM, Kim HJ, et al. Arterial spin-labeling perfusion MRI stratifies progression-free survival and correlates with epidermal growth factor receptor status in glioblastoma. *AJNR American journal of neuroradiology* 2015;36:672-677

36. Ozsunar Y, Mullins ME, Kwong K, et al. Glioma recurrence versus radiation necrosis? A pilot comparison of arterial spin-labeled, dynamic susceptibility contrast enhanced MRI, and FDG-PET imaging. *Acad Radiol* 2010;17:282-290

37. Choi YJ, Kim HS, Jahng GH, et al. Pseudoprogression in patients with glioblastoma: added value of arterial spin labeling to dynamic susceptibility contrast perfusion MR imaging. *Acta Radiol* 2013;54:448-454

38. Valk PE, Dillon WP. Radiation injury of the brain. *AJNR American journal of neuroradiology* 1991;12:45-62

39. Essig M, Shiroishi MS, Nguyen TB, et al. Perfusion MRI: The Five Most Frequently Asked Technical Questions. *Am J Roentgenol* 2013;200:24-34

40. Bagley LJ, Grossman RI, Judy KD, et al. Gliomas: correlation of magnetic susceptibility artifact with histologic grade. *Radiology*

1997;202:511-516

초 록

목적: 랫드 교모세포종 모델에서 역동적 자화 조영 관류 자기공명영상과 동맥 스핀 표지 관류 자기공명영상의 소견과 조직학적 소견과의 비교 분석을 통하여, bevacizumab에 의한 혈관형성억제 효과를 평가하였다.

대상 및 방법: 본 연구는 원내 동물실험윤리위원회의 승인 하에 시행되었다. 교모세포종이 형성된 누드 랫드에서 역동적 자화 조영 관류 자기공명영상과 동맥 스핀 표지 관류 자기공명영상을 시행하였다. 랫드는 무작위적으로 대조군 (n = 4), bevacizumab 치료 후 3 일 군 (n = 6), 치료 후 10 일 군 (n = 6)의 세가지 군으로 나뉘어졌다. 관류 척도들[역동적 자화 조영 관류 자기공명영상에서 얻어진 normalized cerebral blood volume (nCBV), 역동적 자화 조영 관류 자기공명영상에서 얻어진 normalized cerebral blood flow (nCBF), 동맥 스핀 표지 관류 자기공명영상에서 얻어진 normalized cerebral blood flow (nCBF)]과 조직 검사상의 미세혈관영역[microvessel area (MVA)]의 각 군간의 차이는 one-way analysis of variances 를 이용해 분석하였고, 관류 척도와 MVA 사이의 상관 관계는 Pearson 분석을 이용하였다.

결과: 대조군, 치료 후 3 일 군, 치료 후 10 일 군에서 MVA 값은 유의하게 일관된 감소 추이를 보였다. 역동적 자화 조영 관류 자기공명영상에서 얻어진 normalized cerebral blood volume (nCBV), 역동적 자화 조영 관류 자기공명영상에서 얻어진 normalized cerebral blood flow (nCBF), 동맥 스핀 표지 관류 자기공명영상에서 얻어진

normalized cerebral blood flow (nCBF)는 MVA 와 강한 상관 관계를 보였다 ($R^2 = 0.830, 0.755, 0.739$, 모두에서 $P < 0.001$).

결론: 동맥 스핀 표지 관류 자기공명영상에서 얻어진 nCBF 값은 교모세포종에 대한 혈관형성억제 치료의 효과를 평가하는데 유용하다.

주요어: Glioblastoma; Antiangiogenic effect; Bevacizumab; Dynamic susceptibility contrast; Arterial spin labeling.

학 번: 2011-30568